XX IMEKO World Congress
Metrology for Green Growth
September 9–14, 2012, Busan, Republic of Korea

EFFECTS OF INTEGRATING SPHERE CONDITIONS ON THE SPATIAL RESPONSE DISTRIBUTION FUNCTION IN THE TOTAL LUMINOUS FLUX MEASUREMENT

K. Wasapinyokul, R. Leecharoen, S. Chanyawadee, R. Chuenchom, P. Jamparuang, K. Chumpol, C. Charoenkij, and A. Krachangmol

National Institute of Metrology (Thailand), Pathumthani, Thailand, kamol@nimt.or.th

Abstract: The spatial response distribution function of an integrating sphere, for the total luminous flux measurement, was experimentally studied under various conditions. The most apparent effect was the change of signal at the sphere wall around the photo-detector, which typically had higher amplitude than that of the rest. The signal amplitude of such area decreased regarding one of the following conditions: decrease in the reflectance of baffle back surface, decrease in baffle diameter, and increase in the distance between baffle and the detector. The size of area with high amplitude was increased when the aperture diameter of the scanning light increased.

Keywords: Spatial response distribution function, Integrating sphere, Total luminous flux.

1. INTRODUCTION

A method to realise the total luminous flux of a light source, an important photometry parameter, is by the use of an integrating sphere. The principle of this method can be found in typical photometry handbooks [1]. Briefly, the target light source is installed in a hollow sphere, the inner wall of which is coated with a high reflectance material, leading to the multiple diffuse reflection in the sphere if there is a light source inside. Thus the illuminance of the light source, measured from any point on the sphere inner wall, is theoretically constant. The illuminance of the source is detected by a photo-detector located on the sphere inner wall. The electronic signal from the target source is consequently compared with the calibrated signal of a reference source to determine the illuminance of the target. Subsequently the total luminous flux of the target source is calculated.

As the reference and the target sources are often in different characteristics, some correction factors are required in the calculation of the illuminance of target source from that of the reference one. An important correction factor is the spatial correction factor, which identifies how different the luminance distribution of the target and reference sources is. The factor is more crucial when the shapes of both sources are different, e.g. when the target source is a tubular fluorescence lamp while the reference is a spherical incandescent bulb.

The special correction factor is calculated from two parameters [2]: the relative luminous intensity distribution of the internal source and the spatial response distribution function (SRDF). The former is a property of the target source and depends on its shape, while the latter is a specific property of the scanning integrating sphere and strongly depends on sphere scanning conditions. The SRDF is an important parameter of an integrating sphere and relates to the measurement uncertainties of the system [3]. However, experiments to obtain such parameter are time consuming, thus most studies on the parameter are computational [3]. There is a lack of detailed experimental studies of the effect of sphere conditions on the parameter.

In this paper, effects of four scanning parameters on the spatial response distribution function of an integrating sphere are experimentally studied. The parameters studied included the reflectance of the baffle back surface, the baffle diameter, the baffle position, and the diameter of scanning LED aperture. The attention was intensively paid on the sphere inner wall around the detector where the signal had an anomaly profile where it was higher than that of the surrounding areas.

2. EXPERIMENTAL

A sketch of the integrating sphere system used in this experiment is shown in Figure 1. The sphere, made by LMT, had a diameter of 2 m. The right hemisphere is movable for sphere access. The sphere inner wall was coated with LMT photometer paint PHP 80, having a reflectance of 80%. At the centre of the sphere was the scanning LED, a white LED coupled to a lamp post and having an aperture of 20 mm in diameter. The position on the sphere wall, where the LED illuminated, can be controlled from two stepping motors: horizontal and vertical motors, which were remotely controlled by using a computer program to rotate the LED around horizontal (θ) and vertical (ϕ) axes, respectively. The photo-detector was placed at the centre of the left hemisphere. A baffle, whose front and back surfaces were coated with the same PHP 80, 120 mm in diameter, was

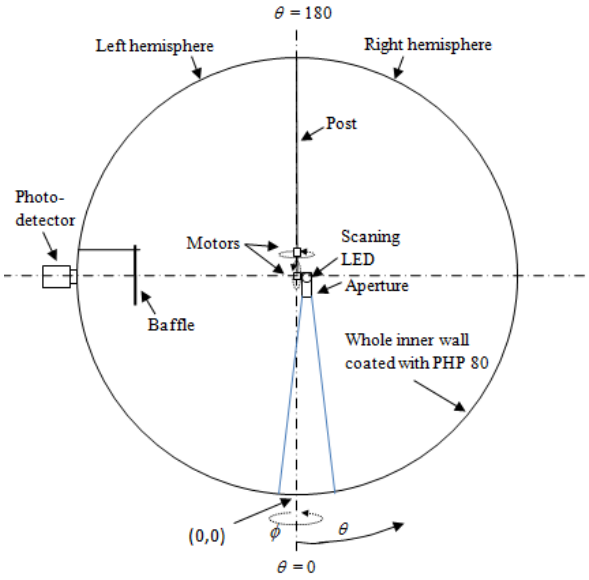

Figure 1: A diagram of the integrating sphere used in the experiment

placed in front of the detector, 250 mm away, to protect the LED light to illuminate directly the photo-detector.

The SRDF of the sphere was determined by using the following procedure. First, the LED was arranged to illuminate at the beginning position, which was at the bottom point of the sphere. At this beginning position, the spherical coordinate, (θ,ϕ), was allocated to be (0,0). The LED was biased at 3.5 V by using a power generator, providing a driven current of 0.17 A. It was left biased at this condition for two hours before the scanning was executed in order for the LED light to be stable. After two hours, the scanning started; the signal from the photo-detector of this beginning position was collected by a computer program. Subsequently, the horizontal motor rotated for one step around the horizontal axis, moving the LED illuminated position from (0,0) to $(\theta_1,0)$, and the detector signal was again collected. The procedure, that the LED was horizontally rotated to illuminate a new position and the signal was collected, was repeated until the illuminated position was the top of the sphere, (180,0). Then the horizontal motor rotated the LED horizontally back to (0,0) while the vertical motor rotated the LED around the vertical axis to be at $(0,\phi_1)$ and the data was again collected. While the vertical axis was at $\phi = \phi_1$, the previous procedure was repeated where the LED was rotated horizontally from $(0,\phi_1)$ to (θ_1,ϕ_1), (θ_2,ϕ_1), and so on, while the data of every step was collected. When the illuminated position reached the top of the sphere, $(180,\phi_2)$, the LED was rotated horizontally and vertically to the position that $\theta = 0$ and new ϕ. Such procedure was repeated until $\phi = 360°$, where (180,360) was the last illuminated position that the data was collected, i.e. the whole inner wall of sphere was scanned. This set of the detector signals is the SRDF profile of the sphere for the given sphere condition. A complete round of scan took 5.5 hours to finish.

To study the effects of sphere conditions on the SRDF, the parameter was collected when one of the following sphere conditions was varied: the reflectance of the baffle back surface, baffle diameter, baffle position, and the size of the scanning LED aperture. Firstly, the reflectance of the baffle back surface was changed by attaching a sheet of paper with different reflectance to the back of the baffle. Three reflectances from three types of baffle back surface were studied: 80% (default baffle with PHP 80), 60% (typical white paper), and 5% (typical black-coloured paper). Secondly, three baffle diameters were studied: 120 mm, 163 mm, and 212 mm. Thirdly, three baffle positions, measured from the detector, were studied: 50 mm, 250 mm, and 450 mm. Lastly, three LED aperture diameters were studied: 10 mm, 20 mm, and 45 mm. While one of these factors was varied, others were kept at their default values, i.e. default baffle (PHP 80, 120 mm diameter, 250 mm away from the detector) and default LED aperture (25 mm diameter). Each scan was taken one day after the previous one was finished where the LED was switched off when there was no scan.

3. RESULTS AND DISCUSSIONS

3.1 SRDF from the default sphere conditions

Figure 2a and 2b show the SRDF of left and right hemisphere, respectively, of the integrating sphere with the default condition, i.e. the baffle was coated with PHP 80, had a diameter of 120 mm, was placed at 250 mm from the detector, and the LED aperture was 20 mm in diameter. The SRDF shown was nominalised by the SRDF of the positions not affected from the baffle or baffle shadow.

The SRDF from the default condition showed expected characteristics. In the right hemisphere, a circular area which had low signal was observed. This was the shadow of the baffle seen by the detector in the opposite side. In the left hemisphere, the signal was low at the centre of the detector, as it was block from the direct incident light by the baffle. However a distinct characteristic was observed around the detector. Typically the signal obtained at this area should be flat and equal to the surrounding areas [1]. In our case, it was stronger than that of the rest. Such characteristic was seen more clearly when the SRDF at $\theta = 90°$ was plotted against ϕ as shown in Figure 3 where the anomaly was

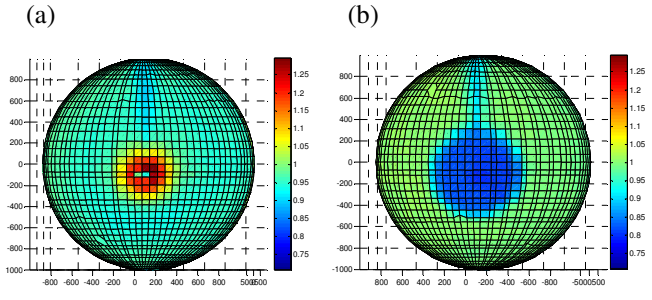

Figure 2: SRDF of (a) left hemisphere, and (b) right hemisphere, of the integrating sphere with default conditions.

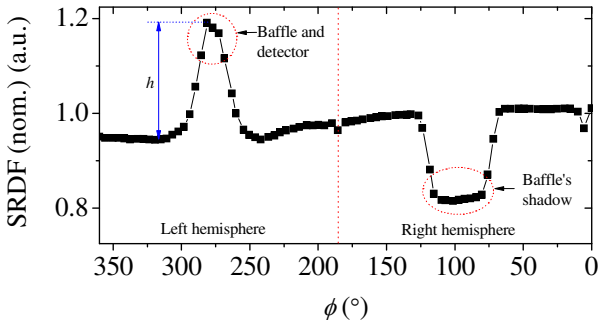

Figure 3: SRDF from Figure 2, at θ = 90°, plotted against ϕ.

shown as a hill with the height of *h*. This characteristic was not found in the works reported by other research groups [1]. The additional signal obtained around the detector was assumed to result from the light reflecting between the sphere wall and the back of the baffle, which was subsequently incident onto the photo-detector, resulting in higher signal amplitude. To study such characteristic more in detail, sphere scanning conditions were varied and the results were discussed in the next sections.

3.2 Effects of the reflectance of the baffle back side on the SRDF

Figure 4a, 4b, and 4c show the SRDF of the sphere wall around the detector (left hemisphere) when the reflectance of the baffle back side was decreased from 80% (default baffle with PHP 80 paint) to 60% (A4 paper), and 5% (black paper), respectively. Figure 4d shows the difference between the signal at the detector area and that of the surrounding areas, *h*, vs the reflectance of the baffle.

For the 80% and 60% reflectances, the SRDFs around the detector had similar trends, where the signal at such area was stronger than that of the surrounding areas, or *h* was a positive value as shown in Figure 4d. Such profile was supposed to result from the reflection of the light incident from the sphere wall to the back of the baffle, which again reflected to the photo-detector, providing a higher signal.

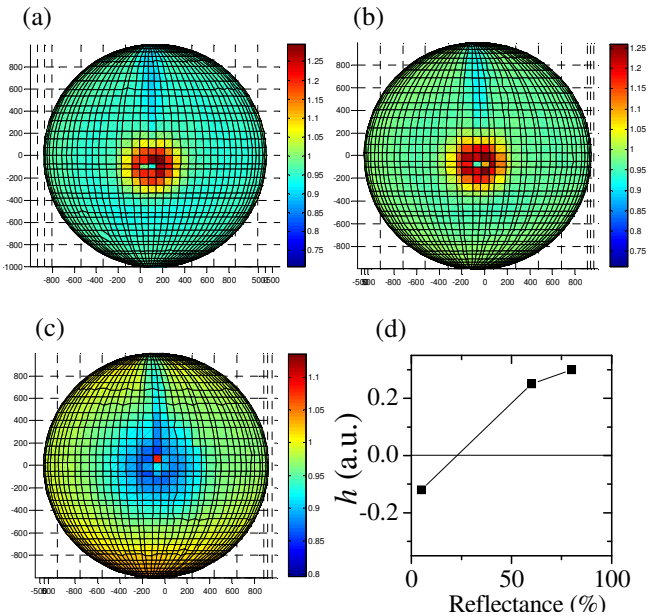

Figure 4: SRDF around the detector when the reflectance of the baffle back surface was (a) 80%, (b) 60%, and (c) 5%; (d) Plot of *h* at different reflectances.

With the 5% reflectance, the trend of profile around the detector was opposite to that of the higher reflectances where it was weaker than that of the surrounding areas, i.e. *h* became negative. This result supported the assumption that such characteristic resulted from the reflection from the back of the baffle. When a black sheet of paper was attached to the back of the baffle, the light reflected from the sphere wall to the baffle was absorbed by the black paper, leading to less light incident onto the photo-detector.

3.3 Effects of the baffle diameter on the SRDF

Figure 5a, 5b, and 5c show the SRDF of the sphere wall around the detector when the baffle diameter was 120 mm, 163 mm, and 212 mm, respectively. Figure 5d shows the plot between the baffle diameter and *h*. All signals had the same trend where the signal amplitude around the detector was higher than that of the surrounding areas (*h* was positive). The effect was more pronounced when a larger baffle was applied. When the 120-mm baffle was applied, *h* was 0.25. The values became 0.8 and 1.2 when the 163-mm and 212-mm baffles, respectively, were applied.

The behaviour, that the height of the signal amplitude around the detector depended on the baffle diameter, can be explained by using the reflection of light from the baffle. With a larger baffle, the light incident on the sphere wall around to the detector had a higher chance to reflect to the detector, hence a stronger signal.

3.4 Effects of the baffle position on the SRDF

Figure 6a and 6b show the SRDF of the sphere wall around the detector when the baffle was placed at 50 mm,

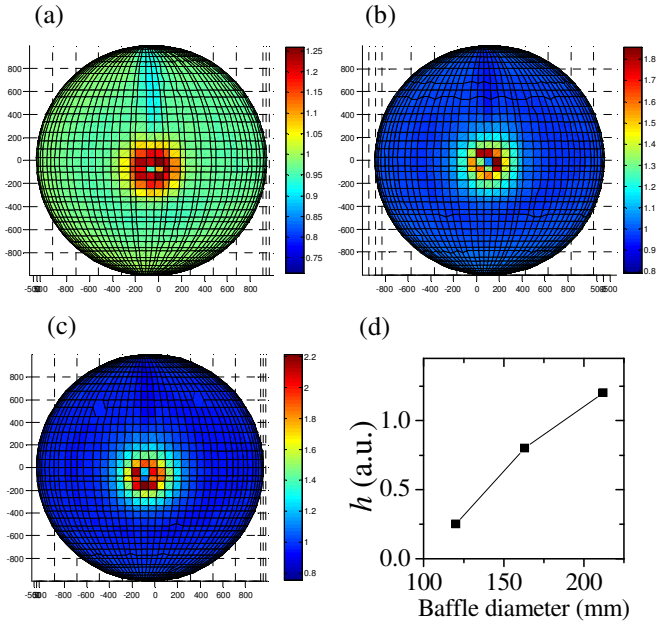

Figure 5: SRDF around the detector when the baffle diameter was (a) 120 mm, (b) 163 mm, and (c) 212 mm; (d) Plot of *h* at different baffle diameter.

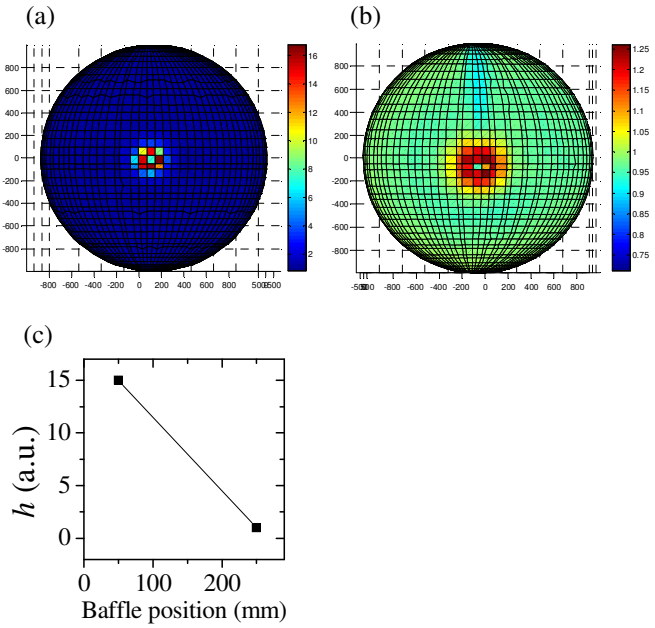

Figure 6: SRDF around the detector when the baffle was (a) 50 mm, and (b) 250 mm, away from the detector; (c) Plot of *h* at different baffle positions.

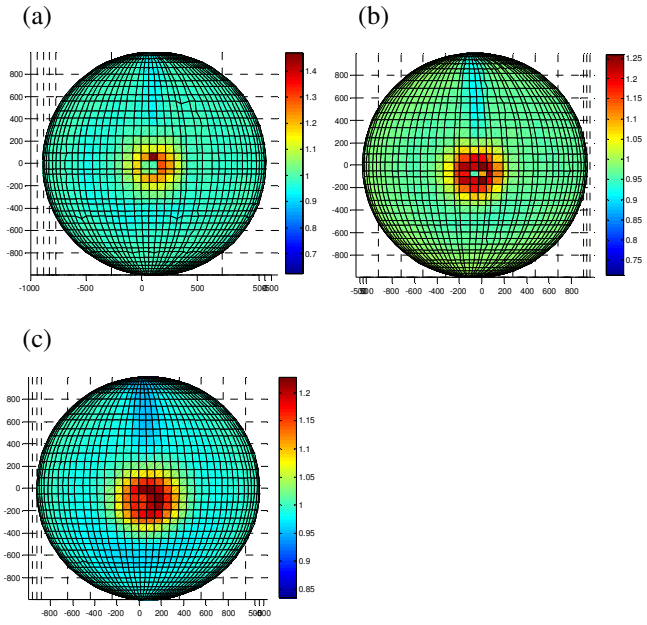

Figure 7: SRDF around the detector when the diameter of scanning LED aperture was (a) 10 mm, (b) 20 mm, and (c) 45 mm.

and 250 mm, respectively, away from the photo-detector. Figure 6c shows the plot between the baffle position and *h*. The SRDF profile obtained from every baffle position had the same behaviour where the signal around the detector was stronger than that of the surrounding areas. This behaviour became more pronounced when the baffle was closer to the detector. At the distance of 50 mm, *h* was ~15. The value decreased to be 0.25 when the distance was 250 mm. This supported the argument that such characteristic was due to the reflection from the back of the baffle. The closer the baffle was to the detector, more reflected photons can be directly incident on the detector.

3.5 Effects of the diameter of scanning LED aperture on the SRDF

Figure 7a, 7b, and 7c show the SRDF when the diameter of the scanning LED aperture was 10 mm, 20 mm, and 45 mm, respectively. All SRDFs had the same characteristic where the signal around the detector was higher than that of the rest (*h* was positive). It was found that a larger aperture provided a larger area with high signal. This can be explained using the relationship between the angle of the light incident on the baffle and the size of the light spot incident on the sphere wall which related to the aperture size. At a small angle, if the light spot was small, the whole spot would be on the baffle. When the light spot became larger, part of the spot would be on the sphere wall close to the back of the baffle, leading to the reflection at the back of the baffle. Thus a larger LED aperture leaded to a larger area around the detector which had high signal of SRDF.

4. CONCLUSIONS

The scanning conditions of an integrating sphere have effects on the SRDF signal of the system. An apparent effect was seen on the signal on the sphere wall around the detector. It was found that the amplitude of the signal at such area was higher than that of the surroundings. This was assumed to result from the light incident on the sphere wall closed to the detector, which subsequently reflected to the back of the baffle and then to the detector, hence a higher signal amplitude. The size of the area which had high signal and the height of the signal amplitude at such area depended on the sphere conditions. The amplitude height decreased regarding one of the following conditions: decrease in the reflectance of the baffle back surface, decrease in the baffle diameter, and increase in the distance between the baffle and the detector. The size of the area which had high signal depended on the aperture size of the scanning light; a bigger aperture provided a larger area which had high signal.

As the SRDF relates to the measurement errors of the total luminous flux measurement [3], the sphere scanning conditions then have direct effects on the measurement uncertainties. By using the information found from this research, the sphere scanning conditions can be optimised to achieve better uncertainties.

5. REFERENCES

[1] C. DeCusatis, Handbook of Applied Photometry. Springer, Ch. 3, pp.82-85, 1997

[2] Y. Ohno, "Realization of NIST 1995 Luminous Flux Scale using Integrating Sphere Method," Journal of Illuminating Engineering Society, vol. 25, no. 1, pp. 13-22, 1996

[3] Y. Ohno, and R. O. Daubach, "Integrating Sphere Simulation on Spatial Nonuniformity Errors in Luminous Flux Measurement," Journal of Illuminating Engineering Society, vol. 30, no. 1, pp. 105-115, 2001